

Scaling Embedding Layers in Language Models

Da Yu[†] Edith Cohen[†] Badih Ghazi[†] Yangsibo Huang[†]
 Pritish Kamath[†] Ravi Kumar[†] Daogao Liu[†] Chiyuan Zhang[†]

Abstract

We propose SCONE (Scalable, Contextualized, Offloaded, N-gram Embedding), a new method for extending input embedding layers to enhance language model performance. To avoid increased decoding costs, SCONE retains the original vocabulary while introducing embeddings for a set of frequent n -grams. These embeddings provide contextualized representation for each input token and are learned with a separate model during training. After training, embeddings are precomputed and stored in off-accelerator memory; during inference, querying them has minimal impact on latency due to the low complexity of embedding lookups. SCONE enables two new scaling strategies: increasing the number of n -gram embeddings and scaling the model used to learn them, both while maintaining fixed accelerator usage during inference (in terms of FLOPS and memory). We show that scaling both aspects enables a model with 1B accelerator-resident parameters to outperform a 1.9B-parameter baseline across diverse corpora, while using only about half the FLOPS and accelerator memory during inference.

1 Introduction

Input embedding layers in language models map discrete tokens to continuous vector representations [47, 54] before passing them to the subsequent layers. Since tokens are typically simple integer values, the mapping can be implemented purely as memory fetch operations with no additional computation needed. This allows embedding layers to be offloaded from the limited and expensive accelerator memory to main memory or even to secondary storage, such as solid-state drives, with minimal impact on inference speed. This is highly desirable, as main memory and secondary storage are significantly more cost-effective than accelerator memory (e.g., GPUs and TPUs) [43]. These advantages motivate us to explore methods for scaling up embedding layers.

However, scaling the embedding layer by simply increasing the token vocabulary size has limited benefits. A larger vocabulary also enlarges the output (logits) layer, whose weight matrix is tied to the vocabulary size and embedding dimension. Typically, predicting the next token requires computing logits over all tokens in the vocabulary, and prior work shows that the decoding cost becomes impractical once the vocabulary exceeds a few hundred thousand tokens [63, 69, 38, 60, 10]. Even if faster hardware or more efficient algorithms might partially offset this cost [31, 56], a second problem remains: scaling the token vocabulary leads to a large number of *tail tokens*, which occur infrequently in the training corpus. The embeddings of these tokens (both input and output) receive very few updates, resulting in lower-quality representations [39, 14]. In Appendix D, we train GPT-2 models with vocabulary sizes ranging from 32K to 2M and observe performance degradation as the vocabulary size exceeds 512K. We attribute this degradation to the increasing sparsity of updates

[†]Google. Correspondence to: {dayuwork,edco,pritishk,chiyuan}@google.com.

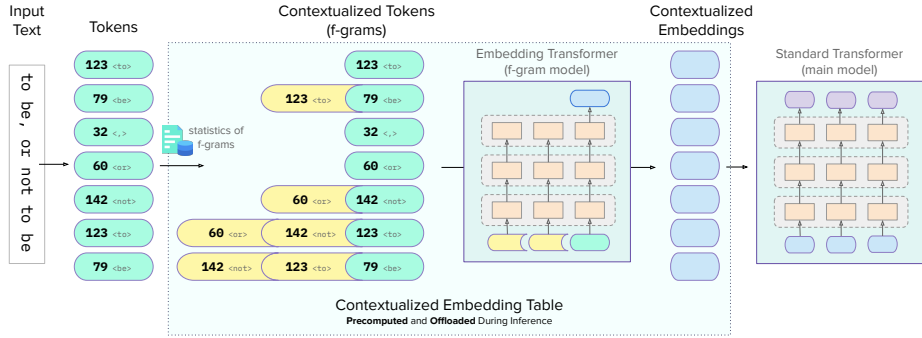


Figure 1: Illustration of SCONE with a maximum n -gram length of 3. The *f-grams* are a set of frequent n -grams selected using the method described in Section 3.1.

per token as the vocabulary grows. Additionally, we observe a linear increase in accelerator memory usage once the vocabulary size exceeds 1M.

Our contributions. In this paper, we propose SCONE, a novel approach for scaling input embedding layers by learning them through a separate transformer model, referred to as the *f-gram model*. This model takes as input a set of frequently occurring n -grams (called *f-grams*), which we select using an approach inspired by Byte-Pair Encoding-based tokenization (Section 3.1). Crucially, the number of f-grams is decoupled from the token vocabulary size, allowing us to build a separate f-gram input embedding table with up to billions of entries, without blowing up the vocabulary size. An overview of the proposed method is illustrated in Figure 1.

During both training and inference, SCONE leverages the f-gram model to efficiently handle large embedding spaces without overwhelming accelerator resources. During training, the f-gram model learns to generate contextualized embeddings for each f-gram without requiring the instantiation of a massive embedding table. During inference, the output of the f-gram model can be precomputed to form the *f-gram embedding layer*. This embedding layer can then be offloaded from the accelerator, thereby eliminating the need for accelerator resources during inference.

SCONE introduces two novel scaling approaches for improving model performance: (i) increasing the number of cached f-gram embeddings and (ii) scaling up the f-gram model used to learn these embeddings. The first approach requires additional off-accelerator memory during inference, while the second demands greater accelerator resources during training. Importantly, both approaches preserve a fixed inference-time accelerator resource footprint, a property *not* supported by traditional scaling methods. Indeed, prior works [30, 24] have shown that scaling the training compute for a fixed model size beyond some compute-optimal threshold leads to diminishing returns. Therefore, the typical method for utilizing additional training compute is to increase model size. However, directly scaling model size also increases FLOPS and accelerator memory requirements during inference. In contrast, SCONE leverages larger f-gram models to effectively consume more accelerator resources during training but without increasing inference-time accelerator demands, offering a novel scaling paradigm that previous studies have not explored.

There are important scenarios where maintaining a fixed inference-time accelerator footprint is especially valuable. In many deployments, where a model is queried billions of times per day, inference costs during deployment can far exceed training costs. In such cases, even small increases in inference-time computation can lead to substantial operational expenses. The recent emergence of test-time scaling techniques further highlights this trend [30, 57], emphasizing situations where inference costs dominate the overall expenses of LLM deployment. Furthermore, many latency-

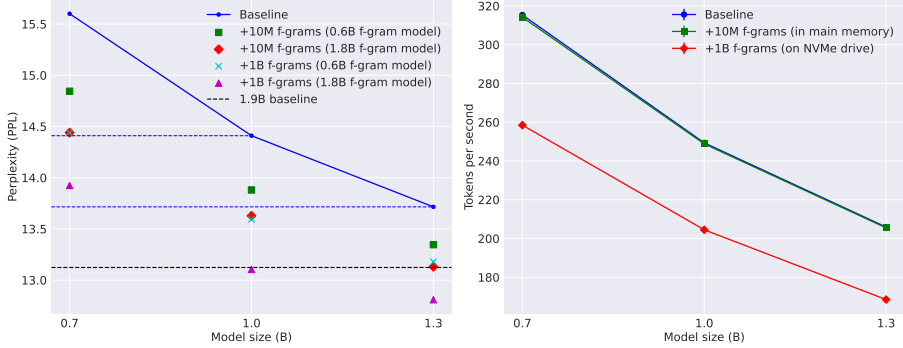


Figure 2: **(Left)** Perplexity on the OLMo [21] evaluation set. Model sizes along the x -axis indicate the number of parameters residing on the accelerator during inference. With 10M f-grams, the 1.3B model matches the performance of the 1.9B baseline; with 1B f-grams, the 1B model surpasses it. **(Right)** End-to-end token generation speed on a single A100 GPU. Storing f-gram embeddings in main memory adds negligible latency, while using NVMe storage introduces a minor slowdown without causing a bottleneck.

sensitive applications impose strict limits on inference-time computation, leaving no margin for increased computational demands during deployment.

Our contributions can be summarized as follows:

- A new scalable method, SCONE, to improve language models by expanding the input embeddings (Section 3) but requiring no additional accelerator resources at inference time.
- Extensive experiments to validate SCONE, analyzing key design choices and their impact on evaluation perplexity and accuracy on downstream tasks (Section 4).

Our results show that SCONE significantly boosts model performance without introducing inference latency bottlenecks; Figure 2 highlights representative findings. Notably, a SCONE model with 1B accelerator-resident parameters outperforms a 1.9B baseline that requires approximately $2\times$ more inference FLOPS and accelerator memory.

2 Preliminaries

We focus on pre-training decoder-only language models with causal language modeling [52]. We now introduce notations that will later help us formally describe the proposed SCONE method. For clarity, we omit details that are not essential to describing our method.

Decoder Transformer Model. Let V_{token} denote the token vocabulary. The *token embedding layer* is parameterized by a function $\mathcal{T} : V_{\text{token}} \rightarrow \mathbb{R}^d$, mapping each token to a d -dimensional embedding vector. We abstract the transformer itself as a function $\mathcal{A} : (\mathbb{R}^d)^{\leq S} \rightarrow \mathbb{R}^d$, which takes as input a sequence of up to S token embeddings and outputs a single embedding vector¹. For completeness, we present the pseudocode of a basic next-token prediction model in Algorithm 2 (Appendix C).

Efficient Indexing for Large Embedding Layers. Mappings from tokens or f-grams to embedding vectors can be implemented as key-value stores, enabling highly efficient lookup. Hash-based and tree-based data structures support lookup times that are constant or logarithmic in the number of entries, respectively. These data structures make it feasible, in principle, to offload large embedding layers from accelerators with minimal impact on latency. In practice, however, the traditional token

¹A decoder transformer typically produces a sequence of embeddings for an input sequence. We define the output as the final token embedding, used either for next-word prediction or as the embedding for a f-gram.

Algorithm 1 SCONE method $F_{\mathcal{T}, V_{\text{f-gram}}, \mathcal{A}_{\text{f-gram}} | \mathcal{F}}$.

- $\mathcal{T} : V_{\text{token}} \rightarrow \mathbb{R}^d$: token embedding layer.
- $V_{\text{f-gram}} \subseteq V_{\text{token}}^{\leq K}$: set of f-grams.
- **Training**: f-gram transformer model
 $\triangleright \mathcal{A}_{\text{f-gram}} : (\mathbb{R}^d)^{\leq K} \rightarrow \mathbb{R}^d$.
- **Inference**: f-gram embedding layer
 $\triangleright \mathcal{F} : V_{\text{f-gram}} \rightarrow \mathbb{R}^d$.

Input: A sequence $(\sigma_1, \dots, \sigma_m) \in V_{\text{token}}^m$ of tokens.
Output: Embeddings $(e_1, \dots, e_m) \in (\mathbb{R}^d)^m$.

for $i = 1, \dots, m$ **do**

$j \leftarrow$ smallest $j' < i$ such that $(\sigma_{j'}, \dots, \sigma_i) \in V_{\text{f-gram}}$ if such a j' exists, otherwise i .

if $j = i$ **then**

$e_i \leftarrow \mathcal{T}(\sigma_i)$

else

$e_i \leftarrow \begin{cases} \mathcal{A}_{\text{f-gram}}(\mathcal{T}(\sigma_j), \dots, \mathcal{T}(\sigma_i)) & \text{at training,} \\ \mathcal{F}(\sigma_j, \dots, \sigma_i) & \text{at inference.} \end{cases}$

return (e_1, \dots, e_m)

embedding layer \mathcal{T} is kept on accelerator memory, as it is typically shared with the output (logits) layer, which requires fast access for matrix multiplications during next-word prediction. In contrast, the f-gram embedding layer introduced by SCONE is decoupled from the output layer and can therefore be offloaded, which is critical for maintaining a fixed accelerator memory footprint as the f-gram layer scales. In Section 4.3, we study two strategies for storing the f-gram embedding table. When stored in main system memory, the f-gram embedding table consists of a dense embedding matrix paired with a hash dictionary that maps f-grams to matrix indices. When stored on NVMe solid-state drives, we use the Lightning Memory-Mapped Database (LMDB) [9] to directly map f-grams to their embeddings using a B+ tree data structure.

3 Scone Architecture

We propose to augment a standard transformer model with an additional f-gram embedding layer. Figure 1 provides a high-level overview of the approach. We first construct a set $V_{\text{f-gram}} \subseteq V_{\text{token}}^{[2, K]} := \bigcup_{n=2}^K V_{\text{token}}^n$ consisting of frequently occurring n -grams of length up to K , which we refer to as *f-grams*. Throughout this paper, K denotes the maximum length of f-grams considered. To construct $V_{\text{f-gram}}$, we use an efficient implementation that requires only $K - 1$ linear scans over the training corpus, as detailed in Section 3.1; the formal construction is described in Algorithm 3 (Appendix C).

Next, we define the SCONE method, which maps a given sequence of tokens to a sequence of embeddings. SCONE behaves differently during training and inference, as described in Algorithm 1. During training, it is parameterized by an f-gram transformer model $\mathcal{A}_{\text{f-gram}} : (\mathbb{R}^d)^{\leq K} \rightarrow \mathbb{R}^d$, which takes an f-gram as input and uses the output embedding of the final token as the embedding for that f-gram. During inference, in contrast, it is parameterized by an f-gram embedding layer $\mathcal{F} : V_{\text{f-gram}} \rightarrow \mathbb{R}^d$, a key-value store that directly maps each f-gram to its precomputed embedding. This embedding layer is implemented by caching the outputs of $\mathcal{A}_{\text{f-gram}}$ for all f-grams in $V_{\text{f-gram}}$ and storing them in off-accelerator memory.

The embeddings produced by SCONE are passed to a standard transformer model $\mathcal{A}_{\text{main}}$, referred

to as the *main model*. This is followed by a prediction head $\mathcal{D} : \mathbb{R}^d \rightarrow \Delta_{V_{\text{token}}}$. Together, these components form the end-to-end process for next-word prediction with SCONE. We present the full description in Algorithm 4 (Appendix C).

In the rest of this section, we will discuss the motivation behind the design choices of SCONE and provide further implementation details.

3.1 BPE-Style Discovery of f-grams

The construction of $V_{\text{f-gram}}$, outlined in Algorithm 3 (Appendix C), can be implemented efficiently with $K - 1$ linear scans over the training corpus. We perform one scan for each $n \in [2, K]$, starting with 2-grams. In subsequent scans, we impose a minimum frequency threshold of 5 to reduce memory usage. At the $(n + 1)$ th scan, the set of n -grams from the previous scan allows us to skip any $(n + 1)$ -gram candidates that cannot meet the minimum threshold. Specifically, if an $(n + 1)$ -gram surpasses the threshold, its n -suffix or prefix must appear at least as many times. Figure 3 shows how the number of unique n -grams (up to 6-grams) grows as the training corpus scales from a few billion to one trillion tokens. Finally, all found n -grams (for $n \in [2, K]$) are ranked by frequency, and the top ones are selected to comprise $V_{\text{f-gram}}$.

Our procedure for counting and ranking n -grams is analogous to continuing the training of a BPE tokenizer on an existing vocabulary. In each BPE iteration [17, 54], the frequencies of all token pairs (2-grams) are counted, and the most frequent pair is merged to form a new token, expanding the vocabulary by one. However, merging and recounting pairs repeatedly to obtain a large number of f-grams is prohibitively expensive for large training corpora. Instead, we simply collect and sort all n -grams up to a small constant K .

3.2 Learning f-gram Embeddings with $\mathcal{A}_{\text{f-gram}}$

We motivate the use of $\mathcal{A}_{\text{f-gram}}$ by contrasting it with the alternative of directly backpropagating gradients to a large embedding table. The direct approach fails to exploit dependencies between n -grams, leading to fewer updates per embedding. We observed this by pretraining GPT-2 models with vocabulary sizes ranging from 32K to 2M. As vocabulary size increases, embedding updates become sparser, eventually degrading performance. For example, when training on 100M tokens, 97.6% of tokens in a 32K vocabulary receive more than 100 updates, compared to only 7.3% in a 2M vocabulary (Appendix D). This sparsity makes it difficult to train a large embedding table through direct gradient updates. SCONE addresses this by parameterizing embeddings with an f-gram transformer $\mathcal{A}_{\text{f-gram}}$, avoiding the sparse update problem.

Additionally, $\mathcal{A}_{\text{f-gram}}$ removes the need to instantiate a full embedding table during training, a requirement that would otherwise strain accelerator memory. This is because, unlike inference, where next-word prediction is largely sequential, training parallelizes computation across the sequence dimension, demanding much higher token throughput. Moreover, during training, embeddings must

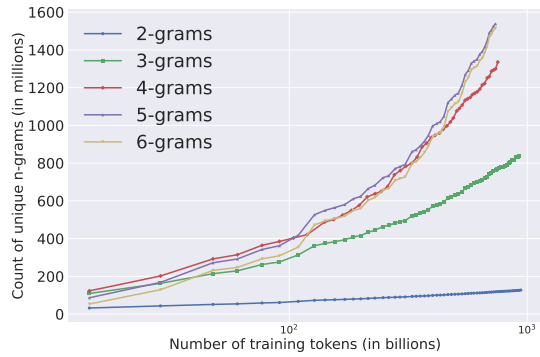


Figure 3: Number of unique 2- to 6-grams appearing at least five times. We uniformly sample tokenized sequences from Dolma [58] to vary the corpus size.

be updated frequently, whereas inference only requires read access. Together, these factors make it difficult to offload the embedding layer from accelerators during training. As a result, avoiding full-table instantiation is crucial for scaling the embedding layer to extremely large sizes.

SCONE jointly trains the $\mathcal{A}_{\text{f-gram}}$ model with the main model $\mathcal{A}_{\text{main}}$ and the token embedding layer \mathcal{T} . This overcomes the sparse updates issue but also introduces additional compute costs. For each $\omega \in V_{\text{f-gram}}$, the computation is the same as that of processing a short sequence of length $|\omega|$ through a standard transformer. Since $|\omega|$ is a small constant, the primary overhead comes from the feed-forward layer. In our experiments (Section 4), we account for this overhead in one of two ways: (1) by training baseline models long enough to reach near-convergence at a fixed model size, ensuring that additional training compute would yield minimal gains; or (2) by reducing the number of training tokens for models using SCONE so that their total training FLOPS match those of the baselines.

During inference, the f-gram embedding layer \mathcal{F} can be precomputed and stored in a lookup table, offloaded to system main memory or secondary storage while still permitting efficient retrieval. Meanwhile, the token embedding layer \mathcal{T} remains on the accelerator for decoding. In Section 4.3, we evaluate the query latency and space usage of the f-gram embedding layer under various configurations. We show that the latency is not a bottleneck for language model inference and the space costs are low due to the use of relatively inexpensive system memory and solid-state drives.

4 Experimental Evaluation

4.1 Design Choices

We analyze three key hyperparameters: (i) the maximum f-gram length K in $V_{\text{f-gram}}$, (ii) the number of f-grams used, $|V_{\text{f-gram}}|$, and (iii) the $\mathcal{A}_{\text{f-gram}}$ model size. We use the released GPT-2 tokenizer, which has $|V_{\text{token}}| = 50,257$, and train on the WebText dataset [50]. The tokenized corpus contains 9B training tokens, from which we extract f-grams using the method in Section 3.1.

We consider three main model sizes with 76M, 340M, and 510M non-embedding parameters. Including the token embedding layer, the total parameter counts increase to 128M, 419M, and 589M, respectively. These models are either trained using only the token embedding layer as a baseline or with an additional $\mathcal{A}_{\text{f-gram}}$ when SCONE is applied. We train all models for 80B tokens, roughly twice the number of training tokens used in Radford et al. [51], to ensure that the baseline models approach convergence. For evaluation, we use the validation split of WebText and WikiText-103 [45], one of the largest downstream datasets in Radford et al. [52]. Additional implementation details are provided in Appendix F.1.

4.1.1 Varying the Maximum f-gram Length

We study the impact of varying the maximum f-gram length K in $V_{\text{f-gram}}$. We vary K from 2 to 8 while keeping the total number of f-grams fixed at 20M. As K increases, the frequency cutoff, which is the minimum number of times an n -gram appears in the training corpus to be included in $V_{\text{f-gram}}$, also increases. The cutoff is 7 when $K = 2$ and 108 when $K = 8$.

For each value of K , we evaluate (i) the model’s perplexity and (ii) the average length of matched f-grams on WikiText-103. The results are shown in Figure 5. We find that evaluation perplexity rises between $K = 2$ and $K = 4$, after which it plateaus with some fluctuations. A similar trend is observed for the average match length, defined as the average length of the f-grams matched by SCONE for each token in the evaluation set. The average match length also increases between $K = 2$ and $K = 4$ and

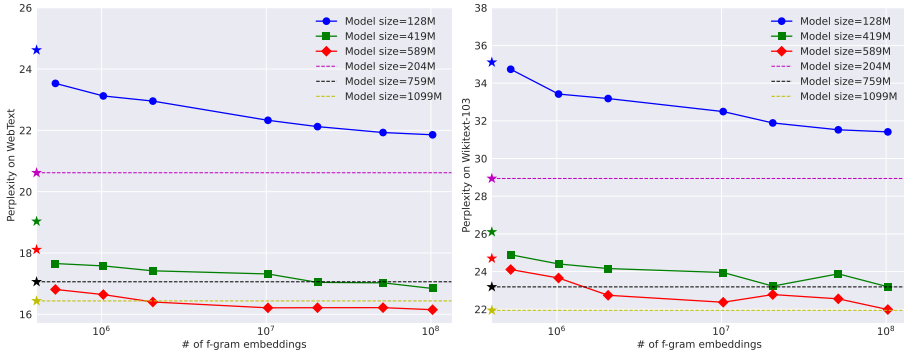


Figure 4: Evaluation perplexity on WebText (left) and WikiText-103 (right) as a function of $|V_{f\text{-gram}}|$. Model sizes in the legend are number of parameters residing on the accelerator during inference. Dashed lines and leftmost stars show baseline performance.

then stabilizes. This trend is likely because longer f-grams are rarer after frequency-based ranking. As a result, even when K is larger, most selected n -grams remain short. Additionally, longer f-grams from the training corpus are less likely to match sequences in downstream data. Experiments on the WebText validation split (Appendix E.1) show a similar trend, although the average match length continues to increase slightly longer, plateauing around $K = 6$.

Considering these findings, for the experiments in the remainder of this paper, we set the maximum f-gram length to $K = 5$ unless stated otherwise.

4.1.2 Varying the Number of f-grams

We observe consistent improvements in language modeling performance as we scale up $|V_{f\text{-gram}}|$. To implement $\mathcal{A}_{f\text{-gram}}$, we replicate the baseline model architecture but remove the token embedding layer. This results in the size of $\mathcal{A}_{f\text{-gram}}$ matches the baseline model’s non-embedding parameters.

Figure 4 shows the evaluation perplexity as $|V_{f\text{-gram}}|$ increases from 512K to 100M. On the WebText validation split, the perplexity decreases consistently as the number of f-gram embeddings increases. Similarly, on WikiText-103, the perplexity generally decreases with more f-gram embeddings, though minor fluctuations are observed.

In Figure 4, we include three additional baselines where the non-embedding parameters of the three main models are doubled, resulting in models with 204M, 759M, and 1099M parameters for the original 128M, 419M, and 589M models, respectively. This ensures that the total parameter count of each baseline matches the training-time parameter count when SCONE is applied. With 100M f-gram embeddings, the 419M and 589M models trained with SCONE match or surpass the performance of the 759M and 1099M baselines, respectively, despite using only half as many non-embedding parameters during inference.

4.1.3 Varying the Size of the $\mathcal{A}_{f\text{-gram}}$ Model

We observe that, for a fixed $|V_{f\text{-gram}}|$, scaling up the $\mathcal{A}_{f\text{-gram}}$ model size provides a new way to improve language modeling performance. We vary the model size by changing the number of layers in the main model architecture. For each $\mathcal{A}_{\text{main}}$ model size, we evaluate four $\mathcal{A}_{f\text{-gram}}$ model sizes: 0.5x, 1x, 2x, and 3x the non-embedding parameters of the main model. We set $|V_{f\text{-gram}}|$ to be 100M. Figure 6 presents the evaluation perplexity on Wikitext-103. The observations on WebText validation split are similar, and we present the results in Appendix E.1.

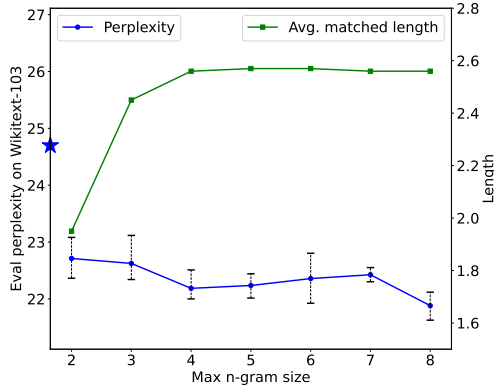


Figure 5: Effect of the maximum f -gram length n on perplexity and matched length. Perplexity decreases as the maximum length increases from 2 to 4, then plateaus with minor fluctuations. Similarly, the average matched length stabilizes after length 4.

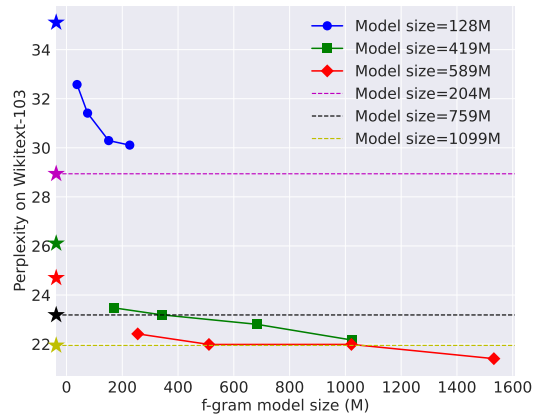


Figure 6: Evaluation perplexity improves as the size of $\mathcal{A}_{f\text{-gram}}$ grows. Model sizes in the legend are main model sizes, including the token embedding layer. Dashed lines and stars on the left represent baselines without an $\mathcal{A}_{f\text{-gram}}$ model.

Table 1: Zero-shot evaluation accuracy on downstream tasks. Models with f -gram embedding layers show clear improvements over the baseline models.

Model	PIQA	HellaSwag	ARC-E	ARC-C	CSQA	MMLU	Avg.
OLMo-1B	73.6	60.9	69.5	31.8	48.7	37.6	53.7 (+0)
OLMo-1.9B	75.3	65.9	74.2	36.8	49.7	38.6	56.8 (+3.1)
OLMo-1B + OE-12.8M [25]	73.7	62.7	70.3	32.1	49.9	37.8	54.4 (+0.7)
OLMo-1B + 10M f -grams	74.0	63.6	70.4	32.1	49.9	39.3	54.9 (+1.2)
OLMo-1.3B + 10M f -grams	75.0	65.5	75.3	36.4	49.9	38.5	56.8 (+3.1)
OLMo-1B + 1B f -grams	75.3	67.1	72.5	36.4	50.8	39.9	57.0 (+3.3)

The results in Figure 6 show that the perplexity generally decreases as the $\mathcal{A}_{f\text{-gram}}$ model size increases, although the improvements become smaller as the model size grows larger. For instance, with the 419M main model, a 170M $\mathcal{A}_{f\text{-gram}}$ model improves the perplexity from 26.1 to 23.4, outperforming the 589M baseline (24.7) by a clear margin. Further scaling of the $\mathcal{A}_{f\text{-gram}}$ model to 1020M (resulting in 1439M total parameters during training) lowers the perplexity to 22.1, which is slightly higher than the 1099M baseline (21.9). This suggests that scaling up the $\mathcal{A}_{f\text{-gram}}$ model initially yields a better scaling curve, but beyond a certain size, it becomes less optimal compared to directly scaling up $\mathcal{A}_{\text{main}}$. However, scaling $\mathcal{A}_{\text{main}}$ also increases accelerator usage during inference, whereas scaling $\mathcal{A}_{f\text{-gram}}$ does not, since it is replaced with an off-accelerator lookup table at inference time. This highlights our method as a novel way to leverage additional training compute while maintaining fixed accelerator usage during inference.

4.2 Scaling Up the Training Corpus

After exploring several design choices for SCONE, we now evaluate its performance in large-scale pretraining. Our implementation builds on the open-source OLMo codebase [21], licensed under Apache 2.0. Additional implementation details are provided in Appendix F.2.

Downstream Tasks. We report zero-shot accuracy on six standard downstream benchmarks: MMLU-var, Hellaswag, ARC-Challenge, ARC-Easy, CommonsenseQA (CSQA), and PIQA. In the main text, we focus on presenting downstream accuracy results under our primary training setting. Additional results, including perplexity evaluations, training curves, and further SCONE configurations under alternative settings, are provided in Appendix E.2. Notably, perplexity trends closely correlate with downstream performance.

Baselines. We compare SCONE against three baselines: OLMo-1B, OLMo-1.9B, and a concurrent method, the over-tokenized transformer [25]. Model configurations for OLMo-1B and OLMo-1.9B are detailed in Appendix F.2. For the over-tokenized transformer, we adopt the best-performing OE-12.8M variant, which introduces an additional input embedding layer comprising 12.8M embedding vectors, applied on top of the OLMo-1B model. Further discussion of this method can be found in Section 5. All baseline models are trained for 1T tokens.

SCONE Configuration. We apply SCONE with two f-gram embedding layer sizes: 10M and 1B f-grams, respectively. The cutoff frequencies are 21,956 for 10M f-grams and 70 for 1B f-grams. SCONE is integrated into OLMo-1B and OLMo-1.3B models, with an $\mathcal{A}_{\text{f-gram}}$ model size of 1.8B parameters (matching the architecture of OLMo-1.9B but excluding the token embedding layer). Models equipped with SCONE are trained for 500B tokens, half the number of tokens used by the baselines, to account for the additional training cost of the $\mathcal{A}_{\text{f-gram}}$ model and ensure comparable total training FLOPS. In Appendix E.2, we also explore a smaller $\mathcal{A}_{\text{f-gram}}$ model of 0.6B parameters, where we observe consistent improvements.

Results. Table 1 presents the downstream accuracy results. Models with SCONE demonstrate clear improvements over the baselines. Specifically, with 10M f-grams, OLMo-1.3B achieves parity with the OLMo-1.9B baseline while using approximately 32% less inference FLOPS and accelerator memory. With 1B f-grams, OLMo-1B slightly outperforms the OLMo-1.9B baseline while requiring approximately 48% less inference FLOPS and accelerator memory. Compared to the over-tokenized transformer, OLMo-1B + 10M f-grams surpasses OLMo-1B + OE-12.8M, which we attribute to the additional capacity introduced by the $\mathcal{A}_{\text{f-gram}}$ model during training.

4.3 Space Usage and Query Latency

We show that the latency of the f-gram embedding layer does not pose a bottleneck at inference, and that system memory and solid-state drives are relatively low-cost.

Table 2: Space usage of the f-gram embedding layer \mathcal{F} , along with unit cost for memory and NVMe solid-state drives [43].

# of n -grams	System memory	Solid-state drive
10^7	41.4 GB	77.3 GB
10^8	413.6 GB	766.8 GB
10^9	(does not fit)	7665.4 GB
Price (per GB)	~ 2 USD	~ 0.1 USD

We experiment with $|V_{\text{f-gram}}|$ being 10M, 100M, and 1B with embedding dimension of $d = 2048$ and 16-bit precision per floating point value. Experiments were conducted on a workstation with 64 Intel Xeon CPU cores and 512 GB of memory. Space and latency were measured for both in-memory and on-disk storage. In memory, embeddings are stored as a single matrix with a hash dictionary

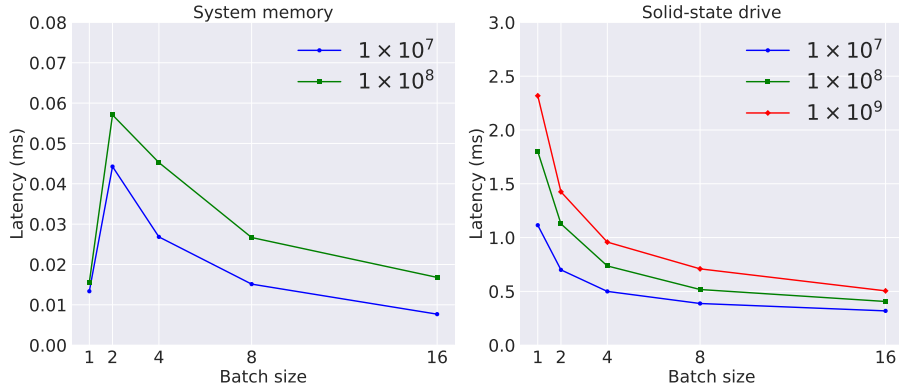


Figure 7: Amortized per-token query latency (ms), averaged over 100,000 batches. The latency spike from batch size 1 to 2 when reading from system memory is due to batch operator overhead, which is less pronounced for solid-state drives.

mapping f-grams to indices, while on-disk storage uses the Lightning Memory-Mapped Database [9] to directly store f-gram and embedding pairs on NVMe solid-state drives.

Table 2 summarizes the space usage for both storage methods. In both cases, the space required increases linearly with the number of embedding vectors. The 10M and 100M f-gram embedding layers are able to fit within main memory, with the 10M layer requiring 41.4 GB. For on-disk storage, there is additional overhead as the same 10M layer occupies 77.3 GB storage.

Figure 7 shows the latency of retrieving embeddings at different batch sizes. Latency is measured as the end-to-end time from loading a batch of tokens to having the f-gram embeddings ready on the GPU. Before each test, the CPU cache is cleared. Up to four queries per token are performed to find the longest matching n -gram (for a maximum n -gram length of $K = 5$). For in-memory storage, sequential queries are sufficient since they are not the bottleneck, whereas on-disk storage uses parallel queries to the database. At a batch size of 1, retrieval from a 10M f-gram embedding layer on NVMe takes 1.1 ms, increasing to 2.3 ms for a 1B-layer: both well below the latency threshold for LLM inference (typical commercial APIs generate at \sim 100 tokens/sec, or \sim 10 ms/token [3]). Larger batch sizes further improve efficiency: at batch size 16, amortized per-token latency drops to 0.5 ms. In-memory access is much faster: for a 100M f-gram layer at batch size 16, per-token latency is only 0.017 ms. We also report end-to-end generation speed in Figure 2, which aligns with these latency trends: when embeddings are stored in main memory, there is negligible impact on throughput; when stored on NVMe drives, throughput slightly decreases but no major bottleneck arises.

5 Related Work

Scaling of Embedding Layers. Prior research on the scalability of embedding layers has primarily focused on token embeddings, where the vocabulary is shared with the language model’s decoding head. For instance, Tao et al. [60] show that larger models benefit from larger vocabularies, reflecting trends where vocabulary sizes have grown from tens of thousands [13, 52] to hundreds of thousands of tokens [20, 1, 15, 40]. However, even for the largest models, the optimal vocabulary sizes predicted by Tao et al. [60] remain much smaller relative to model size. For instance, a vocabulary of 216K tokens for a 70B-parameter model. This relatively small token embedding layer limits the potential for expanding model capacity through token embeddings alone. To address this, Roy et al. [53] propose decoupling input and output embeddings by introducing an additional embedding layer for

bi-grams. Building on this idea, we also decouple the input and decoding embedding layers, but crucially, we parameterize the additional embedding table with a neural network during training. This approach allows us to efficiently scale the additional input embedding layer and introduces a new scaling strategy: scaling the $\mathcal{A}_{\text{f-gram}}$ model that learns to generate the additional embeddings.

Concurrently, Huang et al. [25] propose the over-tokenized transformer, which also decouples input and decoding embeddings by introducing an additional input embedding layer for n -grams. They observe similar performance gains as the input embedding size increases. Unlike our approach, which selectively retains only frequent n -grams, they hash n -grams into a fixed number of embeddings to manage the vast n -gram space, a strategy that likely also mitigates sparse updates (Appendix D). A key distinction is that their additional embedding layer must be fully instantiated and resident on accelerators during training, leading to significant memory challenges despite tensor sharding. Moreover, through the design of $\mathcal{A}_{\text{f-gram}}$, SCONE expands model capacity not only by enlarging the embedding table but also by introducing a scalable $\mathcal{A}_{\text{f-gram}}$ model for learning the embeddings. We compare SCONE with the over-tokenized transformer in Section 4.2. Results suggest that while both SCONE and the over-tokenized transformer show clear improvements over the baseline, SCONE offers better gains owing to the additional capacity provided by $\mathcal{A}_{\text{f-gram}}$.

Mixture of Lookup Experts. A concurrent work by Jie et al. [28] proposes discretizing the inputs to a Mixture-of-Experts (MoE) layer so that, at inference time, it can be implemented as a simple lookup table. They use token embeddings from the input embedding layer as keys for the lookup. This design enables training with a larger MoE layer to improve performance, while having negligible impact on FLOPs and accelerator memory usage during inference. Their approach shares a similar insight with our design of the $\mathcal{A}_{\text{f-gram}}$ model: constructing a neural network module with discretized inputs that can be switched to an efficient lookup table at inference. However, a key difference is that we introduce a method for scaling the number of keys by constructing the set $V_{\text{f-gram}}$. This enables an additional axis of scaling, namely expanding the size of the lookup table at inference. It also allows for fully utilizing the increased model capacity during training. Without this extension, a small number of discretized keys would lead to diminishing returns when scaling the parameters of the discretized module during training.

We discuss additional related work in Appendix B due to space constraints.

6 Conclusion

We introduce SCONE, a scalable approach for generating n -gram contextualized embeddings for each input token. These embeddings are learned during training and cached in off-accelerator storage for inference. SCONE enables two new strategies for scaling language models under fixed inference-time accelerator memory and FLOPS budgets, making it particularly useful for reducing serving costs and supporting latency-sensitive applications.

We discuss limitations and promising directions for future work in Appendix A.

Acknowledgements

The authors would like to thank Andrew Tomkins for his helpful feedback on an early draft.

References

- [1] Bo Adler, Niket Agarwal, Ashwath Aithal, Dong H Anh, Pallab Bhattacharya, Annika Brundyn, Jared Casper, Bryan Catanzaro, Sharon Clay, Jonathan Cohen, et al. Nemotron-4 340b technical report. *arXiv:2406.11704*, 2024.
- [2] Mikel Artetxe, Sebastian Ruder, and Dani Yogatama. On the cross-lingual transferability of monolingual representations. In *ACL*, pages 4623–4637, 2020.
- [3] ArtificialAnlys. Independent analysis of AI models and API providers, 2025. URL <https://artificialanalysis.ai/>. Accessed: 2025-01-07.
- [4] Vincent-Pierre Berges, Barlas Oğuz, Daniel Haziza, Wen-tau Yih, Luke Zettlemoyer, and Gargi Gosh. Memory layers at scale. *arXiv:2412.09764*, 2024.
- [5] Yihong Chen, Bei Chen, Xiangnan He, Chen Gao, Yong Li, Jian-Guang Lou, and Yue Wang. λ opt: Learn to regularize recommender models in finer levels. In *KDD*, pages 978–986, 2019.
- [6] Yihong Chen, Kelly Marchisio, Roberta Raileanu, David Adelani, Pontus Lars Erik Saito Stenetorp, Sebastian Riedel, and Mikel Artetxe. Improving language plasticity via pretraining with active forgetting. In *NeurIPS*, pages 31543–31557, 2023.
- [7] Yihong Chen, Xiangxiang Xu, Yao Lu, Pontus Stenetorp, and Luca Franceschi. Jet expansions of residual computation. *arXiv:2410.06024*, 2024.
- [8] Dokook Choe, Rami Al-Rfou, Mandy Guo, Heeyoung Lee, and Noah Constant. Bridging the gap for tokenizer-free language models. *arXiv:1908.10322*, 2019.
- [9] Howard Chu. Lightning memory-mapped database, 2011. URL <http://www.lmdb.tech/doc/>. Accessed: 2025-01-23.
- [10] Gautier Dagan, Gabriel Synnaeve, and Baptiste Roziere. Getting the most out of your tokenizer for pre-training and domain adaptation. In *ICML*, 2024.
- [11] DeepSpeed. DeepSpeed, 2024. URL <https://github.com/microsoft/DeepSpeed>. Accessed: 2025-01-19.
- [12] Björn Deisereth, Manuel Brack, Patrick Schramowski, Kristian Kersting, and Samuel Weinbach. T-FREE: Subword tokenizer-free generative LLMs via sparse representations for memory-efficient embeddings. In *EMNLP*, 2024.
- [13] Jacob Devlin, Ming-Wei Chang, Kenton Lee, and Kristina Toutanova. Bert: Pre-training of deep bidirectional transformers for language understanding. *arXiv:1810.04805*, 2019.
- [14] Longxu Dou, Qian Liu, Guangtao Zeng, Jia Guo, Jiahui Zhou, Xin Mao, Ziqi Jin, Wei Lu, and Min Lin. Sailor: Open language models for south-East Asia. In *EMNLP*, 2024.
- [15] Abhimanyu Dubey, Abhinav Jauhri, Abhinav Pandey, Abhishek Kadian, Ahmad Al-Dahle, Aiesha Letman, Akhil Mathur, Alan Schelten, Amy Yang, Angela Fan, et al. The Llama 3 herd of models. *arXiv:2407.21783*, 2024.
- [16] William Fedus, Barret Zoph, and Noam Shazeer. Switch transformers: Scaling to trillion parameter models with simple and efficient sparsity. *JMLR*, 2022.
- [17] Philip Gage. A new algorithm for data compression. *The C Users Journal*, 1994.
- [18] Mor Geva, Roei Schuster, Jonathan Berant, and Omer Levy. Transformer feed-forward layers are key-value memories. In *EMNLP*, pages 5484–5495, 2021.
- [19] Mor Geva, Avi Caciularu, Kevin Ro Wang, and Yoav Goldberg. Transformer feed-forward layers build predictions by promoting concepts in the vocabulary space. In *EMNLP*, pages 30–45, 2022.
- [20] Google. Gemma 2: Improving open language models at a practical size. *arXiv:2408.00118*, 2024.

[21] Dirk Groeneveld, Iz Beltagy, Pete Walsh, Akshita Bhagia, Rodney Kinney, Oyvind Tafjord, A. Jha, Hamish Ivison, Ian Magnusson, Yizhong Wang, Shane Arora, David Atkinson, Russell Authur, Khyathi Raghavi Chandu, Arman Cohan, Jennifer Dumas, Yanai Elazar, Yuling Gu, Jack Hessel, Tushar Khot, William Merrill, Jacob Daniel Morrison, Niklas Muennighoff, Aakanksha Naik, Crystal Nam, Matthew E. Peters, Valentina Pyatkin, Abhilasha Ravichander, Dustin Schwenk, Saurabh Shah, Will Smith, Emma Strubell, Nishant Subramani, Mitchell Wortsman, Pradeep Dasigi, Nathan Lambert, Kyle Richardson, Luke Zettlemoyer, Jesse Dodge, Kyle Lo, Luca Soldaini, Noah A. Smith, and Hanna Hajishirzi. OLMo: accelerating the science of language models. In *ACL*, pages 15789–15809, 2024.

[22] Prakhar Gupta, Matteo Pagliardini, and Martin Jaggi. Better word embeddings by disentangling contextual n-gram information. In *NAACL-HLT*, pages 933–939, 2019.

[23] Xu Owen He. Mixture of a million experts. *arXiv:2407.04153*, 2024.

[24] Jordan Hoffmann, Sebastian Borgeaud, Arthur Mensch, Elena Buchatskaya, Trevor Cai, Eliza Rutherford, Diego de Las Casas, Lisa Anne Hendricks, Johannes Welbl, Aidan Clark, et al. Training compute-optimal large language models. *arXiv:2203.15556*, 2022.

[25] Hongzhi Huang, Defa Zhu, Banggu Wu, Yutao Zeng, Ya Wang, Qiyang Min, and Xun Zhou. Over-tokenized transformer: Vocabulary is generally worth scaling. *arXiv:2501.16975*, 2025.

[26] Yuzhen Huang, Jinghan Zhang, Zifei Shan, and Junxian He. Compression represents intelligence linearly. In *COLM*, 2024.

[27] Albert Q Jiang, Alexandre Sablayrolles, Antoine Roux, Arthur Mensch, Blanche Savary, Chris Bamford, Devendra Singh Chaplot, Diego de las Casas, Emma Bou Hanna, Florian Bressand, et al. Mixtral of experts. *arXiv:2401.04088*, 2024.

[28] Shibo Jie, Yehui Tang, Kai Han, Yitong Li, Duyu Tang, Zhi-Hong Deng, and Yunhe Wang. Mixture of lookup experts. In *ICML*, 2025.

[29] Jeff Johnson, Matthijs Douze, and Hervé Jégou. Billion-scale similarity search with GPUs. *IEEE Trans. Big Data*, 2019.

[30] Andy L Jones. Scaling scaling laws with board games. *arXiv:2104.03113*, 2021.

[31] Armand Joulin, Moustapha Cissé, David Grangier, Hervé Jégou, et al. Efficient softmax approximation for GPUs. In *ICML*, pages 1302–1310, 2017.

[32] Yoon Kim, Yacine Jernite, David Sontag, and Alexander Rush. Character-aware neural language models. In *AAAI*, 2016.

[33] Taku Kudo. Sentencepiece: A simple and language independent subword tokenizer and detokenizer for neural text processing. In *EMNLP (Demonstration)*, pages 66–71, 2018.

[34] Taku Kudo. Subword regularization: Improving neural network translation models with multiple subword candidates. In *ACL*, pages 66–75, 2018.

[35] Woosuk Kwon, Zhuohan Li, Siyuan Zhuang, Ying Sheng, Lianmin Zheng, Cody Hao Yu, Joseph E. Gonzalez, Hao Zhang, and Ion Stoica. Efficient memory management for large language model serving with PagedAttention. In *SOSP*, 2023.

[36] Guillaume Lample, Alexandre Sablayrolles, Marc’Aurelio Ranzato, Ludovic Denoyer, and Hervé Jégou. Large memory layers with product keys. In *NIPS*, 2019.

[37] Dmitry Lepikhin, HyoukJoong Lee, Yuanzhong Xu, Dehao Chen, Orhan Firat, Yanping Huang, Maxim Krikun, Noam Shazeer, and Zhifeng Chen. {GS}hard: Scaling giant models with conditional computation and automatic sharding. In *ICLR*, 2021.

[38] Davis Liang, Hila Gonen, Yuning Mao, Rui Hou, Naman Goyal, Marjan Ghazvininejad, Luke Zettlemoyer, and Madian Khabsa. XLM-V: Overcoming the vocabulary bottleneck in multilingual masked language models. In *EMNLP*, 2023.

[39] Xianwen Liao, Yongzhong Huang, Changfu Wei, Chenhao Zhang, Yongqing Deng, and Ke Yi. Efficient estimate of low-frequency words' embeddings based on the dictionary: a case study on Chinese. *Applied Sciences*, 2021.

[40] Aixin Liu, Bei Feng, Bing Xue, Bingxuan Wang, Bochao Wu, Chengda Lu, Chenggang Zhao, Chengqi Deng, Chenyu Zhang, Chong Ruan, et al. Deepseek-v3 technical report. *arXiv:2412.19437*, 2024.

[41] Siyi Liu, Chen Gao, Yihong Chen, Depeng Jin, and Yong Li. Learnable embedding sizes for recommender systems. In *ICLR*, 2021.

[42] Ilya Loshchilov and Frank Hutter. Decoupled weight decay regularization. In *ICLR*, 2019.

[43] John C. McCallum. Price and performance changes of computer technology with time, 2024. URL <https://jcmiit.net/index.htm>. Accessed: 2025-01-20.

[44] Bryan McCann, James Bradbury, Caiming Xiong, and Richard Socher. Learned in translation: Contextualized word vectors. *NIPS*, 2017.

[45] Stephen Merity, Caiming Xiong, James Bradbury, and Richard Socher. Pointer sentinel mixture models. In *ICLR*, 2017.

[46] Meta. Large concept models: Language modeling in a sentence representation space. *arXiv:2412.08821*, 2024.

[47] Tomás Mikolov, Kai Chen, Greg Corrado, and Jeffrey Dean. Efficient estimation of word representations in vector space. In *ICLR (Workshop)*, 2013.

[48] Artidoro Pagnoni, Ram Pasunuru, Pedro Rodriguez, John Nguyen, Benjamin Muller, Margaret Li, Chunting Zhou, Lili Yu, Jason Weston, Luke Zettlemoyer, et al. Byte latent transformer: Patches scale better than tokens. *arXiv:2412.09871*, 2024.

[49] Matthew E. Peters, Mark Neumann, Mohit Iyyer, Matt Gardner, Christopher Clark, Kenton Lee, and Luke Zettlemoyer. Deep contextualized word representations. In *NAACL-HLT*, 2018.

[50] Joshua Peterson, Stephan Meylan, and David Bourgin. Openwebtext, 2019. URL <https://github.com/jcpeterson/openwebtext>. Accessed: 2025-01-19.

[51] Alec Radford, Karthik Narasimhan, Tim Salimans, and Ilya Sutskever. Improving language understanding with unsupervised learning. Technical report, OpenAI, 2018.

[52] Alec Radford, Jeffrey Wu, Rewon Child, David Luan, Dario Amodei, Ilya Sutskever, et al. Language models are unsupervised multitask learners. *OpenAI blog*, 2019.

[53] Aurko Roy, Rohan Anil, Guangda Lai, Benjamin Lee, Jeffrey Zhao, Shuyuan Zhang, Shibo Wang, Ye Zhang, Shen Wu, Rigel Swavely, et al. N-grammer: Augmenting transformers with latent n-grams. *arXiv:2207.06366*, 2022.

[54] Rico Sennrich, Barry Haddow, and Alexandra Birch. Neural machine translation of rare words with subword units. In *ACL*, 2016.

[55] Noam Shazeer, Azalia Mirhoseini, Krzysztof Maziarz, Andy Davis, Quoc Le, Geoffrey Hinton, and Jeff Dean. Outrageously large neural networks: The sparsely-gated mixture-of-experts layer. In *ICLR*, 2017.

[56] Kyuhong Shim, Minjae Lee, Iksoo Choi, Yoonho Boo, and Wonyong Sung. SVD-softmax: Fast softmax approximation on large vocabulary neural networks. In *NIPS*, 2017.

[57] Charlie Snell, Jaehoon Lee, Kelvin Xu, and Aviral Kumar. Scaling LLM test-time compute optimally can be more effective than scaling model parameters. In *ICLR*, 2025.

[58] Luca Soldaini, Rodney Kinney, Akshita Bhagia, Dustin Schwenk, David Atkinson, Russell Author, Ben Bogin, Khyathi Chandu, Jennifer Dumas, Yanai Elazar, Valentin Hofmann, Ananya Jha, Sachin Kumar, Li Lucy, Xinxi Lyu, Nathan Lambert, Ian Magnusson, Jacob Morrison, Niklas Muennighoff, Aakanksha Naik, Crystal Nam, Matthew Peters, Abhilasha Ravichander, Kyle Richardson, Zejiang Shen, Emma Strubell, Nishant Subramani, Oyvind Tafjord, Evan Walsh, Luke Zettlemoyer, Noah Smith, Hannaneh Hajishirzi, Iz Beltagy, Dirk Groeneveld, Jesse Dodge, and Kyle Lo. Dolma: an open corpus of three trillion tokens for language model pretraining research. In *ACL*, 2024.

[59] Sainbayar Sukhbaatar, Jason Weston, Rob Fergus, et al. End-to-end memory networks. *NIPS*, 2015.

[60] Chaofan Tao, Qian Liu, Longxu Dou, Niklas Muennighoff, Zhongwei Wan, Ping Luo, Min Lin, and Ngai Wong. Scaling laws with vocabulary: Larger models deserve larger vocabularies. In *NeurIPS*, 2024.

[61] Hugo Touvron, Louis Martin, Kevin Stone, Peter Albert, Amjad Almahairi, Yasmine Babaei, Nikolay Bashlykov, Soumya Batra, Prajjwal Bhargava, Shruti Bhosale, et al. Llama 2: Open foundation and fine-tuned chat models. *arXiv:2307.09288*, 2023.

[62] Elena Voita, Javier Ferrando, and Christoforos Nalmpantis. Neurons in large language models: Dead, n-gram, positional. In *ACL (Findings)*, pages 1288–1301, 2024.

[63] Hai Wang, Dian Yu, Kai Sun, Jianshu Chen, and Dong Yu. Improving pre-trained multilingual model with vocabulary expansion. In *CoNLL*, 2019.

[64] Junxiong Wang, Tushaar Gangavarapu, Jing Nathan Yan, and Alexander M Rush. MambaByte: Token-free selective state space model. In *COLM*, 2024.

[65] Jason Weston, Sumit Chopra, and Antoine Bordes. Memory networks. *NIPS*, 2015.

[66] Yonghui Wu, Mike Schuster, Zhifeng Chen, Quoc V. Le, Mohammad Norouzi, Wolfgang Macherey, Maxim Krikun, Yuan Cao, Qin Gao, Klaus Macherey, Jeff Klingner, Apurva Shah, Melvin Johnson, Xiaobing Liu, Lukasz Kaiser, Stephan Gouws, Yoshikiyo Kato, Taku Kudo, Hideto Kazawa, Keith Stevens, George Kurian, Nishant Patil, Wei Wang, Cliff Young, Jason Smith, Jason Riesa, Alex Rudnick, Oriol Vinyals, Greg Corrado, Macduff Hughes, and Jeffrey Dean. Google’s neural machine translation system: Bridging the gap between human and machine translation. *arXiv:1609.08144*, 2016.

[67] Linting Xue, Aditya Barua, Noah Constant, Rami Al-Rfou, Sharan Narang, Mihir Kale, Adam Roberts, and Colin Raffel. Byt5: Towards a token-free future with pre-trained byte-to-byte models. *TACL*, 2022.

[68] Lili Yu, Dániel Simig, Colin Flaherty, Armen Aghajanyan, Luke Zettlemoyer, and Mike Lewis. Megabyte: Predicting million-byte sequences with multiscale transformers. *NeurIPS*, 2023.

[69] Bo Zheng, Li Dong, Shaohan Huang, Saksham Singhal, Wanxiang Che, Ting Liu, Xia Song, and Furu Wei. Allocating large vocabulary capacity for cross-lingual language model pre-training. In *EMNLP*, 2021.

A Limitations and Future Work

A promising direction for future work is extending SCONE beyond short n -grams by enabling caching for longer queries. A central challenge lies in designing effective keys for such queries. Using raw text as keys may result in low cache hit rates, as semantically similar queries often vary at the surface level. Alternatively, using semantic embeddings as keys would require discretization techniques to map continuous embeddings into a discrete key space that supports efficient indexing.

One limitation of the current study is that we evaluate SCONE only on models with up to 3B parameters at training time. This constraint is primarily due to hardware limitations, which restrict our ability to conduct large-scale pretraining on larger models. Although the model scales we tested are widely used in real-world applications, exploring the performance of SCONE at larger scales presents an exciting direction for future research. We believe applying SCONE to larger models would be highly beneficial to the community and leave this exploration for future work. Notably, our experiments in Section 4 provide encouraging evidence, as the benefits of SCONE are consistent across all model sizes we tested.

B Additional Related Work

Contextualized Word Embeddings. Words can have different meanings depending on context. Prior work has incorporated context into word embeddings, either from the entire sequence [44, 49] or short n -grams [22], before applying them to downstream tasks. Modern language models inherently use contextualized token embeddings, leveraging attention mechanisms. In this study, we extend the embedding layer to include contextualized f -gram embeddings for each token. A key novelty is that our approach allows embeddings to be precomputed and offloaded from accelerators, providing contextual embeddings for each token without increasing FLOPS and accelerator memory usage at inference.

Tokenization in Language Models. Our method assumes a predefined vocabulary from a trained tokenizer. Several popular algorithms exist for training tokenizers [54, 66, 34, 33]. In this work, we use a BPE tokenizer, following prior seminal works [52, 61]. However, our method is not tied to any specific tokenization algorithm and can be applied seamlessly to others.

Tokenization-free language models have also been widely explored [32, 8, 67, 68, 64, 12, 46, 48]. While we have not tested our method on tokenization-free models, we believe our core idea—introducing an off-accelerator embedding layer by precomputing embeddings for frequent input patterns—remains applicable.

Mixture-of-Experts (MoE) and Memory Layers. MoE and memory layers are two established approaches for scaling language models within a fixed FLOPS budget.

MoE layers replace traditional feedforward layers with multiple parallel “experts,” activating only one or a few per token using a lightweight routing mechanism [55, 37, 16, 27, 23]. This allows the model to scale by increasing the number of experts without increasing the computational cost per token. However, all experts must reside on the accelerator, resulting in significantly higher memory usage.

Memory layers, on the other hand, store large collections of embeddings (continuous vectors) and retrieve the nearest neighbors during the forward pass via (approximate) similarity search [65, 59, 36, 4]. These retrieved embeddings enhance the model’s capabilities without adding much to the FLOPS

Algorithm 2 Basic Next-Word Prediction Model $M_{\mathcal{T}, \mathcal{A}, \mathcal{D}}$.

Parameters:

- $\mathcal{T} : V_{\text{token}} \rightarrow \mathbb{R}^d$: token embedding layer,
- $\mathcal{A} : (\mathbb{R}^d)^{\leq T} \rightarrow \mathbb{R}^d$: transformer model, where T is the maximum sequence length,
- $\mathcal{D} : \mathbb{R}^d \rightarrow \Delta_{V_{\text{token}}}$: prediction head.

Input: $(\sigma_1, \dots, \sigma_m) \in V_{\text{token}}^*$ for $m \leq T$.**Output:** Probability distribution over next token $\hat{\sigma}_{m+1}$.**for** $i = 1, \dots, m$ **do** $e_i \leftarrow \mathcal{T}(\sigma_i)$: Input embedding per token. $e_{\text{out}} \leftarrow \mathcal{A}(e_1, \dots, e_m)$: Output embedding.**return** $D(e_{\text{out}})$

budget. Despite improvements in similarity search techniques [36, 29], memory layers still require storing the embeddings on the accelerator, making memory demands impractically high at larger scales [4]. Furthermore, because embeddings are typically updated via backpropagation, memory layers introduce additional challenges related to sparse updates as the memory size grows.

While MoE layers, memory layers, and our proposed method SCONE all maintain fixed inference FLOPS, a key advantage of SCONE is it also maintains fixed accelerator memory usage at inference. By focusing on the input embedding layer, SCONE ensures that the computational overhead remains $O(1)$ during inference and enables offloading the additional parameters off-accelerator with negligible impact on end-to-end latency.

Implicit n -gram Patterns in Transformers. Recent work analyzing the internal mechanisms of transformers has shown that these models often utilize implicit n -gram patterns for prediction [18, 19, 62]. For instance, Chen et al. [7] demonstrate that certain attention heads can detect specific n -gram patterns, while MLPs can perform linguistic operations such as adding the “-ing” suffix. These findings underscore the importance of n -gram information in language modeling and offer a potential explanation for the effectiveness of SCONE. An interesting future direction is to examine how SCONE’s f-gram embeddings interact with the transformer’s implicit n -gram patterns.

Embedding Sparsity in Multilingual Applications and Recommender Systems. This work focuses on a common setting for training LLMs: language modeling on large-scale text corpora, primarily in English. However, scaling embedding layers presents challenges beyond this context, particularly due to frequency-related performance degradation caused by sparsity. Multilingual applications are one such scenario. Two phrases in different languages may refer to the same concept but correspond to different embedding vectors. Their embeddings should ideally be close. Recent work has explored methods for learning transferable embeddings in cross-lingual settings [2, 6]. Another relevant example is scaling the embeddings for recommender systems [5, 41], where embeddings often dominate the model’s parameter count due to the high cardinality of user or item categories. For both scenarios, SCONE’s strategy, i.e., parameterizing large embedding tables using a neural network, provides a complementary approach to help mitigate sparsity issues.

C Additional Algorithms

In Section 2, we discuss a simple next-word prediction model, $M_{\mathcal{T}, \mathcal{A}, \mathcal{D}}$, consisting of a token embedding layer \mathcal{T} , a transformer model \mathcal{A} , and a prediction head \mathcal{D} . This model takes a token

Algorithm 3 Constructing a set of f-grams $V_{\text{f-gram}}$.

Parameters: S : desired size of $V_{\text{f-gram}}$.

Input: $\{(\sigma_1, \dots, \sigma_T)^{(i)}\}$: token sequences from training set.

Output: $V_{\text{f-gram}} \subseteq V_{\text{token}}^{[2, K]}$: set of f-grams of size S .

for $n = 2, \dots, K$ **do**

for $\omega := (\sigma'_1, \dots, \sigma'_k) \in V_{\text{token}}^n$ **do**

$C_\omega \leftarrow$ the number of times ω appears in all sequences $\{(\sigma_1, \dots, \sigma_T)^{(i)}\}$.

Let $\omega_1, \omega_2, \dots$ be list of elements of $\bigcup_{n=2}^K V_{\text{token}}^n$, sorted such that $C_{\omega_1} \geq C_{\omega_2} \geq \dots$, breaking ties arbitrarily.

return $\{\omega_1, \dots, \omega_S\}$: set of f-grams of size S .

Algorithm 4 Next-word prediction with SCONE $M_{\mathcal{T}, V_{\text{f-gram}}, \mathcal{A}_{\text{f-gram}} | \mathcal{F}, \mathcal{A}_{\text{main}}, \mathcal{D}}$

Parameters:

- $\mathcal{T} : V_{\text{token}} \rightarrow \mathbb{R}^d$: token embedding layer,

- $V_{\text{f-gram}} \subseteq V_{\text{token}}^{[2, K]}$: set of f-grams,

- **Training:** f-gram transformer model

$\triangleright \mathcal{A}_{\text{f-gram}} : (\mathbb{R}^d)^{\leq K} \rightarrow \mathbb{R}^d$,

- **Inference:** f-gram embedding layer

$\triangleright \mathcal{F} : V_{\text{f-gram}} \rightarrow \mathbb{R}^d$.

- $\mathcal{A}_{\text{main}} : (\mathbb{R}^d)^{\leq T} \rightarrow \mathbb{R}^d$: main transformer model.

- $\mathcal{D} : \mathbb{R}^d \rightarrow \Delta_{V_{\text{token}}}$: Prediction head.

Input: $(\sigma_1, \dots, \sigma_m) \in V_{\text{token}}^*$ for $m \leq T$, where T is the maximum sequence length.

Output: Probability distribution over next token $\hat{\sigma}_{m+1}$.

$(e_1, \dots, e_m) \leftarrow F_{\mathcal{T}, V_{\text{f-gram}}, \mathcal{A}_{\text{f-gram}} | \mathcal{F}}(\sigma_1, \dots, \sigma_m)$ (Algorithm 1)

$e_{\text{out}} \leftarrow \mathcal{A}_{\text{main}}(e_1, \dots, e_m)$

return $D(e_{\text{out}})$

sequence $(\sigma_1, \dots, \sigma_m)$, with each token from the token vocabulary V_{token} , and produces a probability distribution for the next token. We provide the pseudocode for $M_{\mathcal{T}, \mathcal{A}, \mathcal{D}}$ in Algorithm 2.

In Section 3, we introduce an algorithm for constructing a set of f-grams given a target number of f-grams. We present the pseudocode for the construction process in Algorithm 3. Although Algorithm 3 clearly illustrates the procedure, it is too expensive to implement in practice. In Section 3.1, we describe an efficient implementation that requires only $K - 1$ linear scans over the pre-training corpus, where K is a hyperparameter controlling the maximum length of f-grams.

In Algorithm 1 in Section 3, we present the pseudocode for SCONE’s process of generating contextualized f-gram embeddings. Next, we describe the end-to-end next-word prediction process using SCONE (Algorithm 4). Specifically, the process, denoted as $M_{\mathcal{T}, V_{\text{f-gram}}, \mathcal{A}_{\text{f-gram}} | \mathcal{F}, \mathcal{A}_{\text{main}}, \mathcal{D}}$, takes an input sequence $(\sigma_1, \dots, \sigma_m) \in V_{\text{token}}^*$ and produces a distribution over the next token $\hat{\sigma}_{m+1}$. Note that in Algorithm 4, f-gram embeddings are generated with $\mathcal{A}_{\text{f-gram}}$ during training and retrieved from a lookup table \mathcal{F} during inference.

D Challenges of Scaling Vocabulary Size in Embedding Layers

Scaling the token vocabulary size is the most straightforward way to enlarge an embedding layer, but we find that larger token vocabularies degrade performance beyond a certain threshold and

significantly increase accelerator usage during decoding. We pre-train GPT-2 models [52] with three sizes of non-embedding parameters: 85M (small), 302M (medium), and 708M (large) on the WebText dataset [50], testing six vocabulary sizes ranging from 32,768 to 2,097,152. The tokenizers are trained using the BPE algorithm [17, 54]. We follow the implementation in Tao et al. [60], which allows token merges across word boundaries. Each model is trained on 80B tokens. Since larger vocabularies produce fewer tokens for the same dataset, they effectively enable models to process more data. Additional implementation details such as training hyperparameters are provided in Appendix F.1.

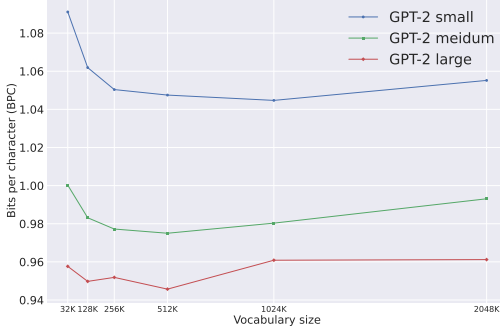


Figure 8: BPC of three model sizes on the validation set (lower is better). For all three model sizes, BPC initially improves as vocabulary size increases but eventually deteriorates.

Figure 8 presents the average bits per character (BPC) on the WebText validation set. We report BPC instead of cross-entropy loss because the latter is sensitive to vocabulary size, with larger vocabularies typically producing higher losses. BPC, by contrast, is a common vocabulary-insensitive metric for comparing models trained with different tokenizers [26]. We observe that BPC for all three models initially improves with larger vocabulary sizes but eventually deteriorates.

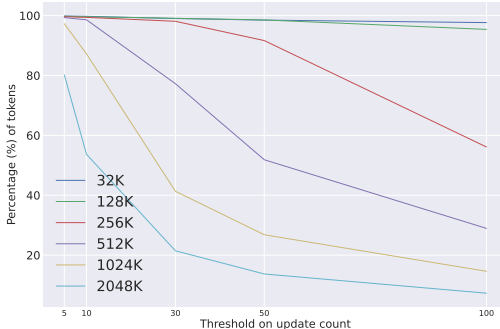


Figure 9: Percentages of tokens (y -axis) that receive more than a given number of updates (x -axis), measured over 100M training tokens. As the vocabulary size increases, tokens receive increasingly sparse updates.

Figure 9 shows the percentages of tokens that receive more than a given number of updates over 100M training tokens. In standard embedding layers, gradients are directly backpropagated to the embedding vectors. With a fixed number of training tokens, larger vocabularies lead to fewer updates per token. For a vocabulary size of 2,097,152, only 7.3% of tokens receive more than 100 updates, compared to 97.6% for a vocabulary size of 32,768. This suggests that the performance drop for larger vocabularies may stem from sparse updates to per-token embedding vectors.

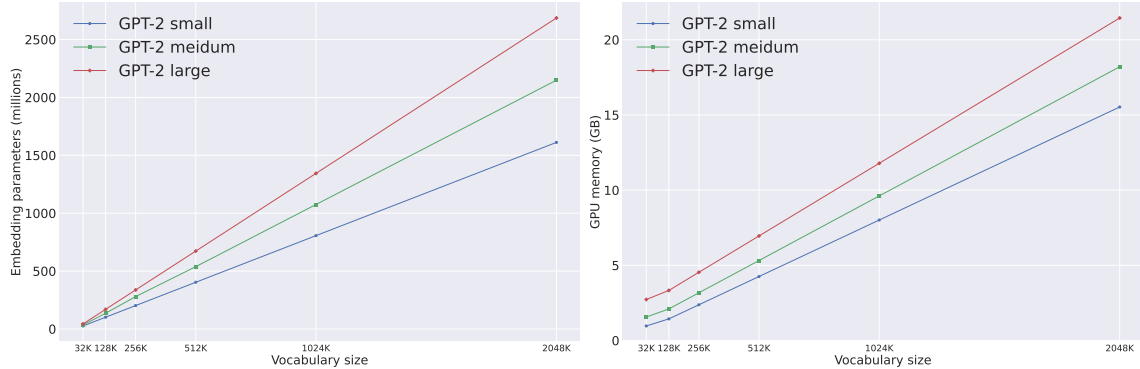


Figure 10: Number of embedding layer parameters stored on GPU and the corresponding memory usage. For large vocabulary sizes, the memory usage increases linearly with the vocabulary size.

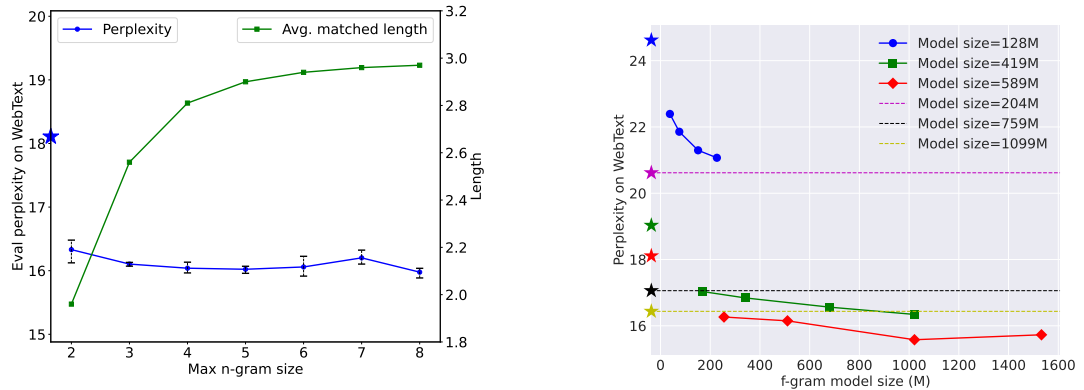


Figure 11: Effect of the maximum f-gram length in $V_{f\text{-gram}}$, evaluated on the WebText validation split.

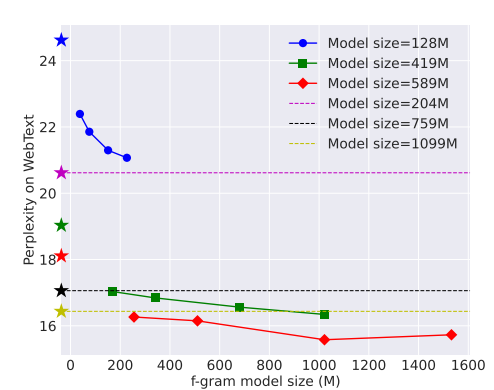


Figure 12: Evaluation perplexity on WebText as a function of the size of $\mathcal{A}_{f\text{-gram}}$.

In addition to performance degradation, increasing the vocabulary size significantly raises accelerator usage during the inference stage. This is because predicting the next token involves running a linear layer and softmax operation across the entire vocabulary to identify the closest embedding. Figure 10 illustrates that both the number of embedding layer parameters stored on the GPU and the GPU memory cost increase linearly with vocabulary size. These costs are measured using a batch size of 1, a sequence length of 1024, and 16-bit precision.

E Additional Experiments

E.1 More Results for Training on WebText

Varying Maximum f-gram Length. In Section 4.1.1, we discuss the impact of varying the maximum f-gram length in $V_{f\text{-gram}}$ and present results on Wikitext-103. We observe that a relatively small maximum length is sufficient, as long as it is not too small, otherwise, the number of available n -grams for ranking becomes too limited. Here, in Figure 11, we show the corresponding results on WebText, which exhibit similar trends. The left y -axis represents the evaluation loss (averaged over three seeds), with the leftmost star indicating baseline performance. The right y -axis shows the

average length of matched f-grams. As the maximum size increases, the loss initially decreases but then plateaus with some fluctuations. Meanwhile, the matched length rises initially before stabilizing for larger values.

Varying $\mathcal{A}_{\text{f-gram}}$ Model Size. In Section 4.1.3, we discuss the impact of varying the size of $\mathcal{A}_{\text{f-gram}}$ on evaluation perplexity for Wikitext-103. We find that increasing the model size leads to further performance improvements for a fixed $|V_{\text{f-gram}}|$. In Figure 12, we present the results on WebText, which show a similar trend. Model sizes in the legend correspond to inference-time sizes on accelerators. Dashed lines and stars on the left represent baseline performance. The evaluation perplexity improves as the size of $\mathcal{A}_{\text{f-gram}}$ grows.

E.2 Additional Results for Training on the OLMo Corpus

We present training curves and perplexity evaluations for models trained on the OLMo corpus. For SCONE, we introduce an additional $\mathcal{A}_{\text{f-gram}}$ model size of 0.6B, alongside the 1.8B $\mathcal{A}_{\text{f-gram}}$ model discussed in Section 4.2. Due to the large number of experiments, all models in this section are trained for 200B tokens, constrained by computational resources. This differs from Section 4.2, where SCONE-enabled models are trained for 500B tokens and baseline models for 1T tokens.

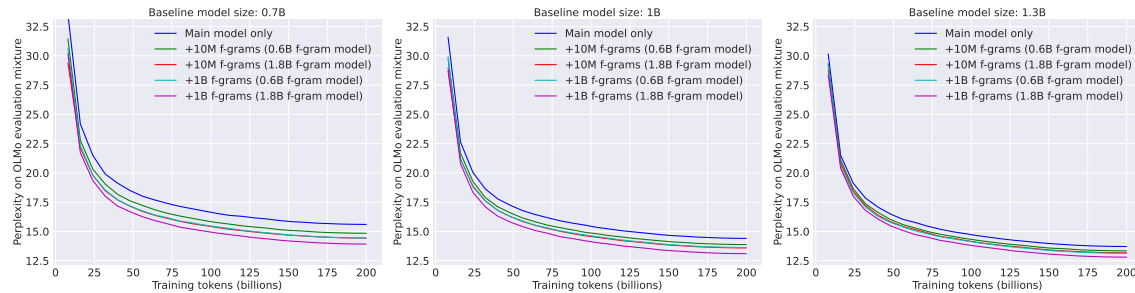


Figure 13: Average perplexity on the OLMo evaluation mixture throughout training. Models with SCONE enabled converge later, indicating stronger capacity, and achieve better perplexity.

Training Curves. Figure 13 shows the evaluation perplexity curves for OLMo-0.7B, OLMo-1B, and OLMo-1.3B throughout training. The curves indicate that models trained with SCONE converge more slowly, suggesting that SCONE effectively increases model capacity. Furthermore, both increasing the number of f-grams and enlarging the $\mathcal{A}_{\text{f-gram}}$ model size enhance model capacity.

Perplexity Evaluation. Figure 2 presents perplexity results on the OLMo evaluation mixture², which covers 11 diverse corpora, including web crawl data, literature, online forums, scientific writing, coding, and more. Table 3 details the performance breakdown by corpus. Results show that increasing both $|V_{\text{f-gram}}|$ and the size of $\mathcal{A}_{\text{f-gram}}$ consistently improves performance across all datasets.

Additionally, Figure 2 reports token generation speeds measured using the vLLM framework [35] with a batch size of 1. Even with large $|V_{\text{f-gram}}|$, embedding retrieval remains efficient and is not a bottleneck for inference.

As a representative example, in the 1B model variant, the baseline achieves an average perplexity of 16.082. Setting $|V_{\text{f-gram}}|$ to 10M improves perplexity to 15.459 with a 0.6B $\mathcal{A}_{\text{f-gram}}$ model and

²<https://github.com/allenai/OLMo/blob/v0.4.0/configs/official/OLMo-1B.yaml#L90>

Table 3: SCONE consistently improves perplexity (lower is better) across all evaluation corpora. We train three baseline models with sizes of 1B, 1.3B, and 1.9B parameters. For the 1B and 1.3B baseline models, we apply SCONE using four different configurations and present the results directly below each corresponding baseline.

Model size	c4-en	books	common-crawl	pes2o	reddit	stack	wiki	ice	m2de-s2orc	pile	wikitext-103	Average
1B baseline	16.813	21.570	16.752	11.682	22.612	3.360	14.453	15.281	27.900	10.429	16.053	16.082
+10M V_f -gram (0.6B \mathcal{A}_f -gram)	16.087	20.963	16.039	11.270	21.797	3.274	13.777	14.979	26.361	10.128	15.371	15.459
+10M V_f -gram (1.8B \mathcal{A}_f -gram)	15.727	20.429	15.473	11.124	21.388	3.231	13.454	14.709	25.785	9.956	15.104	15.125
+1B V_f -gram (0.6B \mathcal{A}_f -gram)	15.846	20.593	15.684	11.071	21.411	3.213	13.543	14.702	26.026	9.889	15.077	15.187
+1B V_f -gram (1.8B \mathcal{A}_f -gram)	15.158	19.680	14.857	10.761	20.757	3.133	12.964	14.220	24.958	9.553	14.354	14.581
1.3B baseline	15.994	20.157	15.921	11.148	21.634	3.248	13.721	14.651	26.583	9.927	15.143	15.284
+10M V_f -gram (0.6B \mathcal{A}_f -gram)	15.509	19.816	15.407	10.887	21.022	3.192	13.260	14.372	25.450	9.757	14.616	14.844
+10M V_f -gram (1.8B \mathcal{A}_f -gram)	15.193	19.587	14.995	10.795	20.735	3.171	13.071	14.272	25.258	9.674	14.438	14.654
+1B V_f -gram (0.6B \mathcal{A}_f -gram)	15.270	19.510	15.106	10.707	20.763	3.139	13.073	14.177	25.009	9.546	14.397	14.609
+1B V_f -gram (1.8B \mathcal{A}_f -gram)	14.803	18.996	14.541	10.502	20.296	3.085	12.637	13.971	24.533	9.357	13.971	14.245
1.9B baseline	15.270	19.017	15.184	10.719	20.752	3.163	13.119	14.095	25.461	9.570	14.229	14.598

to 15.125 with a 1.8B \mathcal{A}_f -gram model—the latter outperforming the 1.3B baseline (15.284). Further increasing $|V_f$ -gram| to 1B improves perplexity to 15.187 (0.6B \mathcal{A}_f -gram) and 14.581 (1.8B \mathcal{A}_f -gram), surpassing the 1.9B baseline (14.598) while requiring only about half the FLOPS and accelerator memory at inference time.

F Implementation Details

We provide additional implementation details below. Most of our experiments are conducted on 4 8×H100 nodes, while some experiments are conducted on 2 16×A100 nodes.

While f-gram lookup is efficient for inference, it creates a bottleneck during training since at training time transformer models process all token positions in parallel. This leads to GPU idle time when fetching the longest matching f-gram on the fly. To remove this bottleneck, after we construct the set of f-grams (V_f -gram), we pre-scan the training sequences to tag the longest matching length for each token. During training, we can then directly retrieve the corresponding f-gram for forward computation with the \mathcal{A}_f -gram model.

For the \mathcal{A}_f -gram model, we use an absolute position embedding layer where the maximum position equals the longest n -gram in V_f -gram. Within each batch, all f-grams are padded to the longest n -gram length in that batch. We train all models with the bfloat16 precision.

F.1 WebText

For pre-training on WebText [50], we follow Radford et al. [52] and set the batch size and sequence length to 512 and 1024, respectively. Radford et al. [52] do not specify the number of training tokens or optimizer details. We train the models for 80B tokens, roughly doubling the count in Radford et al. [51]. For optimization, we use AdamW [42] with a weight decay of 0.1. Following Hoffmann et al. [24], we set the maximum learning rate to 2×10^{-4} and apply a cosine learning rate scheduler. We list the model configurations in Table 4.

Parameters (M)	d_model	ffw_size	n_layers
128	1024	4096	6
204	1024	4096	12
491	1536	6144	12
759	1536	6144	24
589	1536	6144	18
1099	1536	6144	36

Table 4: Baseline model configurations for pre-training on WebText. For constructing the f-gram model ($\mathcal{A}_{\text{f-gram}}$), we vary the number of layers in the 128M, 491M, and 589M variants and discard the token embedding layer.

Parameters (M)	d_model	ffw_size	n_layers
711	2048	8192	12
1014	2048	8192	18
1316	2048	8192	24
1920	2048	8192	36

Table 5: Model configurations for pre-training on the OLMo corpus. To construct the f-gram model ($\mathcal{A}_{\text{f-gram}}$), we use the 711M and 1920M variants, excluding the token embedding layers.

F.2 OLMo Tokenized Training Corpus

For pre-training on the OLMo tokenized training corpus, we follow the optimizer settings for the 1B variant in Groeneveld et al. [21]³. All models use a sequence length of 2048. We use DeepSpeed [11] with ZeRO stage 1 that partitions the optimizer state across GPUs to reduce GPU memory usage. We list the model configurations in Table 5.

³<https://github.com/allenai/OLMo/blob/v0.4.0/configs/official/OLMo-1B.yaml#L40>